The structure of singularities in nonlocal transport equations

2008 J. Phys. A: Math. Theor. 41 185204

(http://iopscience.iop.org/1751-8121/41/18/185204)

J. Phys. A: Math. Theor. **41** (2008) 185204 (12pp) doi:10.1088/1751-8113/41/18/185204

The structure of singularities in nonlocal transport equations

F de la Hoz[1] **and M A Fontelos**[2]

[1] Departamento de Matemática Aplicada, Universidad del País Vasco-Euskal Herriko Unibertsitatea, Escuela Universitaria de Ingenierí a Técnica Industrial, Plaza de la Casilla 3, 48012 Bilbao, Spain
[2] Instituto de Matemáticas y Física Fundamental, Consejo Superior de Investigaciones Científicas, C/ Serrano 123, 28006 Madrid, Spain

Received 5 January 2008, in final form 26 March 2008
Published 18 April 2008
Online at stacks.iop.org/JPhysA/41/185204

Abstract
We describe the structure of solutions developing singularities in the form of cusps in finite time in nonlocal transport equations of the family:

$$\theta_t - \delta(\theta H(\theta))_x - (1-\delta)H(\theta)\theta_x = 0, \qquad 0 \leqslant \delta \leqslant 1, \quad (1)$$

where H represents the Hilbert transform. Equations of this type appear in various contexts: evolution of vortex sheets, models for quasi-geostrophic equation and evolution equations for order parameters. Equation (1) was studied in [1] and [2], and the existence of singularities developing in finite time was proved. The structure of such singularities was, nevertheless, not described. In this paper, we will describe the geometry of the solution in the neighborhood of the singularity once it develops and the (self-similar) way in which it is approached as $t \to t_0$, where t_0 is the singular time.

PACS numbers: 02.30.Jr, 02.60.Cb, 02.60.Nm

(Some figures in this article are in colour only in the electronic version)

1. Introduction

We present some results on partial differential equations (PDEs) of transport type for a scalar θ with nonlocal velocities or fluxes. We concentrate on the case of one space dimension, and the nonlocal operator will be given by the Hilbert transform of θ defined as

$$H\theta(x) = \frac{1}{\pi} PV \int_{-\infty}^{\infty} \frac{\theta(y)}{x-y}\,\mathrm{d}y \quad (2)$$

or

$$H\theta(x) = \frac{1}{2\pi} PV \int_{-\pi}^{\pi} \frac{\theta(x-y)}{\tan\frac{y}{2}}\,\mathrm{d}y, \quad (3)$$

in the periodic case. Nonlocal transport equations appear in various contexts and, in all of them, a central question is the appearance of singularities during the evolution and the mathematical description of such singularities. The simplest transport equation developing singularities (in the form of shocks) in finite time is the Burgers equation:

$$\theta_t + \theta\theta_x = 0.$$

The simplest nonlocal analogs result in the replacement of the transport velocity θ by $-H\theta$ in the flux of θ or in velocity:

$$\theta_t - (H(\theta)\theta)_x = 0 \tag{4}$$

and

$$\theta_t - H(\theta)\theta_x = 0. \tag{5}$$

Equation (4) appears as a formal 1D analog to the 2D quasi-geostrophic equation (QG), which models the dynamics of the mixture of cold and hot air and the fronts between them, and reads

$$\begin{aligned} &\theta_t + (u \times \nabla)\theta = 0, \\ &u = \nabla^{\perp}\psi, \quad \theta = -(-\Delta)^{\frac{1}{2}}\psi, \\ &\theta(x,0) = \theta_0(x), \end{aligned} \tag{6}$$

where $\nabla^{\perp} = (-\partial_2, \partial_1)$. Here, $\theta(x,t)$ represents the temperature of the air. Besides its direct physical significance [6, 10], the quasi-geostrophic equation has very interesting features of resemblance to the 3D Euler equation, the finite time blow-up for QG also being an outstanding open problem. With respect to this question, there are pioneering studies by Constantin *et al* [5]. There are many studies on the equations following that work [9, 11, 13]. The analogy with (4) comes from the fact that

$$u = -\nabla^{\perp}(-\Delta)^{-\frac{1}{2}}\theta = -R^{\perp}\theta, \tag{7}$$

and hence

$$\theta_t + \operatorname{div}[(R^{\perp}\theta)\theta] = 0, \tag{8}$$

where we have used the notation $R^{\perp}\theta = (-R_2\theta, R_1\theta)$ with R_j, $j = 1, 2$, for the two-dimensional Riesz transform defined by (see e.g. [12])

$$R_j(\theta)(x,t) = \frac{1}{2\pi} PV \int_{\mathrm{R}^2} \frac{(x_j - y_j)\theta(y,t)}{|x-y|^3}\,\mathrm{d}y. \tag{9}$$

The equivalent (in terms of homogeneity) singular integral operator to the Riesz transform in 1D is the Hilbert transform. Therefore, (4) is just (8) with $R^{\perp}(\cdot)$ replaced by $-H(\cdot)$ and $\operatorname{div}(\cdot)$ replaced by ∂_x.

As mentioned above, equation (5) represents the simplest case of a transport equation with a nonlocal velocity. It is well known that the equivalent equation with a local velocity $v = \theta$, known as Burger's equation, may develop shock-type singularities in finite time. Therefore, a natural question to pose is whether the solutions to (5) become singular in finite time or not. In fact, this question has been previously considered in the literature motivated by the strong analogy with the Birkhoff–Rott equation modeling the evolution of a vortex sheet, where a crucial mathematical difficulty lies in the nonlocality of the velocity.

The analogy of (5) with Birkhoff–Rott equations was first established in [4] and [8]. These are integrodifferential equations modeling the evolution of vortex sheets with surface tension.

The system can be written in the form

$$\frac{\partial}{\partial t} z^*(\alpha, t) = \frac{1}{2\pi \mathrm{i}} PV \int \frac{\tilde{\gamma}(\alpha')\, \mathrm{d}\alpha'}{z(\alpha, t) - z(\alpha', t)}, \tag{10}$$

$$\frac{\partial \tilde{\gamma}}{\partial t} = \Sigma \kappa_\alpha, \tag{11}$$

where $z(\alpha, t) = x(\alpha, t) + \mathrm{i}y(\alpha, t)$ represents the two-dimensional vortex sheet parametrized with α and κ denotes mean curvature. Following [4] we substitute, in order to build up the model, equation (10) by its 1D analog

$$\frac{\mathrm{d}x(\alpha, t)}{\mathrm{d}t} = -H(\theta), \tag{12}$$

where we have identified $\gamma(\alpha, t)$ with θ. In the limit of $\sigma = 0$ in (11) we conclude that γ is constant along trajectories and this fact leads, in the 1D model, to the equation

$$\theta_t - (H\theta)\, \theta_x = 0.$$

Another interesting context in which transport equations with nonlocal velocities arise is in evolutionary PDEs for geometric order parameters (see [7]). These equations can be of the form

$$\frac{\partial \rho}{\partial t} = -\mathrm{div}\, \mathbf{J},$$

where $\mathbf{J}$ is proportional to ρ and to quantities involving (in general) convolutions of ρ with certain kernels, that is, velocities given in the form of integral operators of ρ. An interesting question concerning this class of PDEs is the existence of solutions involving localized singularities, sometimes called peakons or cuspons, that develop and propagate.

Problems of the type (4), (5) were already studied in [4] and [8]. In [8] the following equation was considered that generalizes (4) and (5), including them as particular cases (when $\delta = 1$ and $\delta = 0$ respectively):

$$\theta_t - \delta(H(\theta)\theta)_x - (1 - \delta)H(\theta)\theta_x = 0 \qquad \text{with} \quad 0 \leqslant \delta \leqslant 1. \tag{13}$$

In [2], we proved the existence of singularities for the full range of $0 < \delta \leqslant 1$. The proof of existence of singularities in the case $\delta = 0$ is solved in [1] using a different technique. The singularities have the form of cusps that develop at the local maxima of θ (see figure 1). Our purpose in the present paper is to describe the structure of the solutions close to the singularities and the shape of the cusps depending on the value of the parameter δ.

In section 2, we study the case $\delta = 1$ in detail and describe the self-similar structure of the singularities developing in finite time. In section 3, we describe the singularities that develop in the range $0 < \delta < 1$. The limit case $\delta = 0$ represents a singular limit of the case $\delta > 0$ and we will briefly discuss the singularities in this case in section 4. Finally, section 5 will be devoted to the description of the numerical method used for the numerical results in previous sections.

2. The case $\delta = 1$

In the case $\delta = 1$, one gets the equation

$$\theta_t - (\theta H(\theta))_x = 0, \tag{14}$$

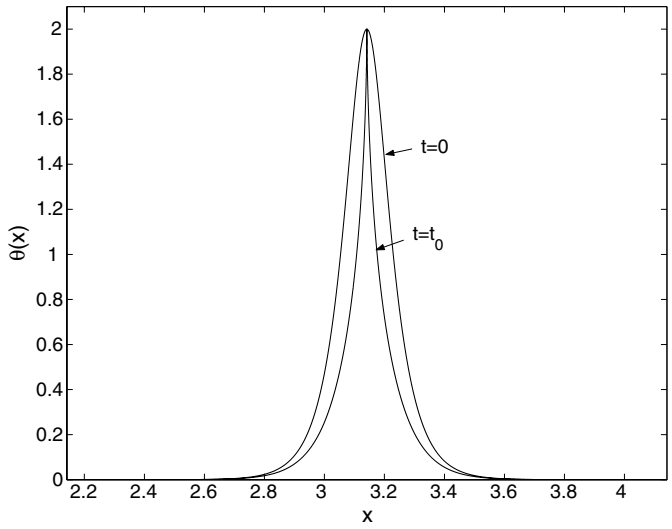

Figure 1. Profiles of θ for $\delta = 0$ at times $t = 0$ and $t = t_0$ where t_0 is the time of formation of the singularity. The initial datum is $\theta(x, 0) = 2\mathrm{sech}(15(x - \pi))$.

and applying Hilbert transform to (16) and using the following properties of Hilbert transform:

$$H(Hf) = -f,$$
$$H(fHg + gHf) = (Hf)(Hg) - fg,$$
$$(Hf)_x = H(f_x),$$

we deduce the equation

$$(H\theta)_t - \tfrac{1}{2}((H\theta)^2 - \theta^2)_x = 0 \tag{15}$$

that can be combined with (14) into a single equation for $z = H\theta + \mathrm{i}\theta \equiv u + \mathrm{i}\theta$:

$$z_t - zz_x = 0,$$

for which one can find the following solution $\theta(x, t)$ (see [2] for details on its deduction) given implicitly by

$$t\theta = \ln\sqrt{\theta^2 + u^2}, \tag{16}$$
$$(x - tu) = \arctan\frac{\theta}{u}. \tag{17}$$

This solution corresponds to an initial datum $\theta(x, 0) = \sin(x)$ and develops singularities at $x = \frac{\pi}{2}$, $t = e^{-1}$ and $\theta = e$, $u = 0$. We shall describe next the local structure of the solution near the singularity. In order to do that, we write

$$t = e^{-1} + t', \qquad \theta = e + \theta',$$
$$u = u', \qquad x = \frac{\pi}{2} + x',$$

which introduced into (16), (17) together with

$$u' = (-t')^{\frac{1}{2}}U, \quad \theta' = (-t')^{\frac{1}{2}}\Theta, \quad x' = (-t')X$$

lead, at leading order and for $t' \to 0$, to

$$-e = \tfrac{1}{2}e^{-2}U^2 + \tfrac{1}{2}e^{-2}\Theta^2 - \Theta^2 e^{-2},$$
$$0 = eX - U\Theta e^{-1},$$

and we conclude

$$\Theta = e^{\frac{3}{2}} \sqrt{1 + \sqrt{1 + \left(\frac{X}{e}\right)^2}} \equiv e^{\frac{3}{2}} \Theta_{ss}\left(\frac{X}{e}\right), \tag{18}$$

$$U = e^{\frac{3}{2}} \frac{X/e}{\sqrt{1 + \sqrt{1 + \left(\frac{X}{e}\right)^2}}} \equiv e^{\frac{3}{2}} (H\Theta_{ss})\left(\frac{X}{e}\right). \tag{19}$$

Thus, the solutions near the singularity are self-similar with profiles given by (18), (19).

More generally, we can provide with a local analysis near a singularity developing at (x_0, t_0). Assume that θ_0 is the value of θ at (x_0, t_0). We write

$$\theta = \theta_0 - B(t_0 - t)^{\frac{1}{2}} \Theta_{ss}\left(\frac{X}{\theta_0}\right) + \widetilde{\theta}, \tag{20}$$

with Θ_{ss} as the self-similar profile defined by (18) and hence satisfying (using also (19))

$$-\tfrac{1}{2}\Theta_{ss} + X\Theta_{ss,X} - \theta_0 (H\Theta_{ss,X}) = 0,$$

and $\widetilde{\theta}$ assumed to be $o((t_0 - t)^{\frac{1}{2}})$. Then one can compute at leading order in $(t_0 - t)$ the following equation for $\widetilde{\theta}$:

$$\widetilde{\theta}_t - \theta_0 (H\widetilde{\theta})_x - B^2 (\Theta_{ss} H\Theta_{ss})_X = 0. \tag{21}$$

Since $\Theta_{ss} H\Theta_{ss} = -X/\theta_0$, we immediately deduce the following solution of (21):

$$\widetilde{\theta} = -B^2 \theta_0^{-1} (t_0 - t).$$

Therefore, near a singularity the solution behaves in the form (see figures 2, 3)

$$\theta(x, t) = \theta_0 - B(t_0 - t)^{\frac{1}{2}} \Theta_{ss}\left(\frac{X}{\theta_0}\right) - B^2 \theta_0^{-1} (t_0 - t) + o(t_0 - t).$$

When $t \to t_0$, the cusp behaves locally near x_0 in the form

$$\theta(x, t_0) \sim \theta_0 - B\theta_0^{-\frac{1}{2}} |x - x_0|^{\frac{1}{2}}.$$

In the following sections, we shall provide numerical experiments showing this behavior for arbitrary initial data.

3. The case $0 < \delta < 1$

In this case, we can write the equation in the form

$$\theta_t - \delta\theta H(\theta_x) - H(\theta)\theta_x = 0, \tag{22}$$

so that one has under symmetry and at the maximum of θ the equation

$$\theta_{\max,t} = \delta \; H(\theta_x)|_{x_{\max}} \theta_{\max},$$

implying, in general, variation of the value of the maximum of θ. Let us call θ_0 the value of θ at the singular point, say $x_0 = 0$, when the singularity develops, say at t_0. Close to that point we introduce $\theta = \theta_0 + \varepsilon\widetilde{\theta}$ and get, after linearization, the equation

$$\widetilde{\theta}_t - \delta\theta_0 H(\widetilde{\theta}_x) = 0.$$

Introducing the new variable $y = x/\delta\theta_0$ and the property $H(H\widetilde{\theta}) = -\widetilde{\theta}$, we deduce

$$\widetilde{\theta}_t - H(\widetilde{\theta}_y) = 0 \qquad \text{and} \qquad (H\widetilde{\theta})_t + \widetilde{\theta}_y = 0. \tag{23}$$

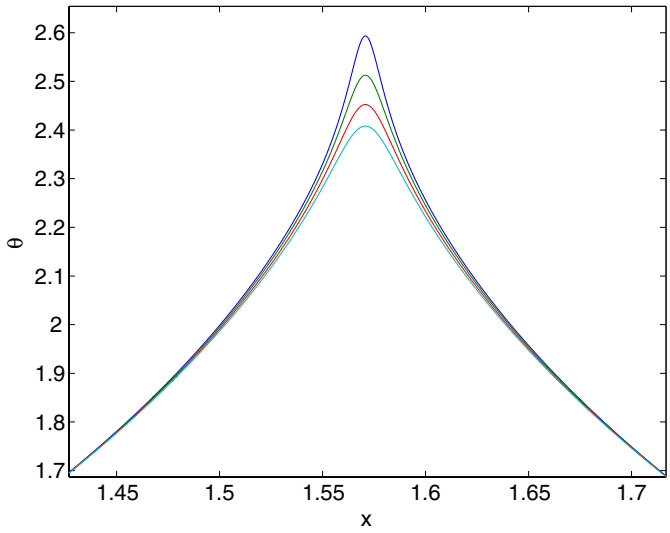

Figure 2. Profiles $\theta(x,t)$ taken in the neighborhood of $x = \frac{\pi}{2}$ and at times $t = 10^{-4}, 2 \times 10^{-4}, 3 \times 10^{-4}, 4 \times 10^{-4}$, from the time of formation of the singularity. The equation has been solved numerically for initial data $\theta(x,0) = \sin(x)$.

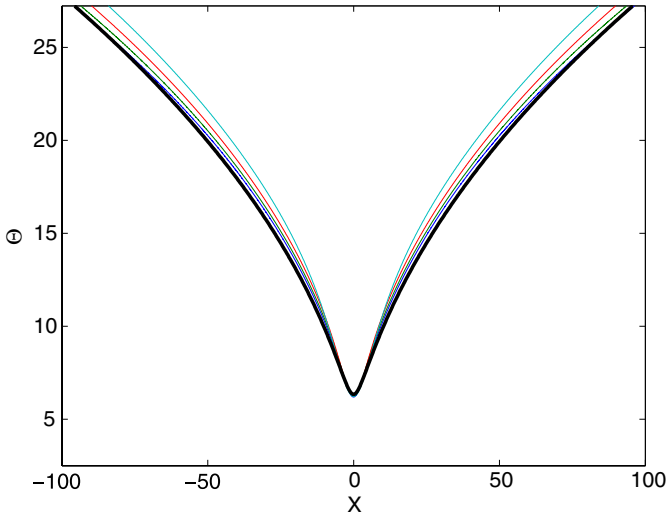

Figure 3. The same profiles $\theta(x,t)$ as in figure 2, but rescaled according to formulae (18) and (20). The thick line corresponds to the theoretical profile (18).

Equation (23) is equivalent to

$$\widetilde{\theta}_{tt} + \widetilde{\theta}_{yy} = 0,$$

from which it is simple to deduce self-similar solutions in the form of separable solutions in polar coordinates. Namely, by introducing $r = \sqrt{(t_0 - t)^2 + y^2}$ and $\tan\theta = \frac{y}{t_0 - t} \equiv Y$, we can

construct solutions in the form

$$\widetilde{\theta} = \mathrm{Re}(z^\alpha) = r^\alpha \cos(\alpha\theta) = (t_0 - t)^\alpha (1 + Y^2)^{\frac{\alpha}{2}} \cos(\alpha \arctan Y) \equiv (t_0 - t)^\alpha \Theta_{ss}(Y), \tag{24}$$

and since (23) constitutes a Cauchy–Riemann system for $\widetilde{\theta}$ and $H\widetilde{\theta}$ we have

$$\begin{aligned} H\widetilde{\theta} &= \mathrm{Im}(z^\alpha) = r^\alpha \sin(\alpha\theta) \\ &= (t_0 - t)^\alpha (1 + Y^2)^{\frac{\alpha}{2}} \sin(\alpha \arctan Y) \equiv (t_0 - t)^\alpha (H\Theta_{ss})(Y). \end{aligned} \tag{25}$$

Note that in the particular case $\alpha = \frac{1}{2}$, we have

$$(1 + Y^2)^{\frac{1}{4}} \cos\left(\tfrac{1}{2} \arctan Y\right) = \tfrac{1}{\sqrt{2}}\left(1 + (1 + Y^2)^{\frac{1}{2}}\right)^{\frac{1}{2}},$$

an expression identical, up to multiplicative constants, to (18).

Guided by the result in the previous section for $\delta = 1$, we shall seek solutions of the form

$$\theta(x, t) = \theta_0 + (t_0 - t)^\alpha \Theta\left(X \equiv \frac{x}{(t_0 - t)}\right) + (t_0 - t)^{2\alpha} G\left(X \equiv \frac{x}{(t_0 - t)}\right). \tag{26}$$

This ansatz for θ implies

$$\begin{aligned} &\theta_t = (t_0 - t)^{\alpha-1}(-\alpha\Theta + X\Theta') + (t_0 - t)^{2\alpha-1}(-2\alpha G + XG'), \\ &(\theta H(\theta))_x = (t_0 - t)^{\alpha-1}\theta_0 (H\Theta)' + (t_0 - t)^{2\alpha-1}(\Theta H\Theta)' + (t_0 - t)^{2\alpha-1}\theta_0 HG', \\ &H(\theta)\theta_x = (t_0 - t)^{2\alpha-1} H\Theta(\Theta)' + (t_0 - t)^{3\alpha-1}(\Theta HG' + GH\Theta'), \end{aligned}$$

which introduced into (22) lead, at order $O((t_0 - t)^{\alpha-1})$, to the equation $(-\alpha\Theta + X\Theta') - \delta\theta_0 (H\Theta)' = 0$, satisfied by the self-similar solution Θ_{ss} (defined in (24)), and, at order $O((t_0 - t)^{2\alpha-1})$, to the equation

$$(-2\alpha G + XG') - \theta_0 \delta HG' - \delta(\Theta H\Theta)' - (1 - \delta)(H\Theta)\Theta' = 0. \tag{27}$$

We cannot integrate equation (27) but provide numerical evidence below showing how the similarity exponents α (which appear to be independent of initial data) depend on δ. The details on the numerical method are given in the last section of the paper. As the main result, we found that the exponent α increases slowly from values close to zero (for δ close to zero) up to $\frac{1}{2}$ (which is the analytical result for $\delta = 1$ obtained in the previous section). This implies the formation of cusps such that $\theta \sim \theta_0 - C|x - x_0|^{\alpha(\delta)}$ with $0 < \alpha(\delta) \leqslant \frac{1}{2}$. The case $\delta = 0$ represents a singular limit that will be treated in the following section.

In figure 4 we represent, for $\delta = \frac{1}{2}$, the maximum of $\kappa = |\theta_{xx}|$ raised to some power γ (that is, κ^γ) as a function of time. We have chosen γ in such a way that the resulting curve fits as well as possible to a straight line. A linear behavior for κ^γ would imply that $\kappa \simeq A(t_0 - t)^{\frac{1}{\gamma}}$. Given the similarity law represented by (26) that would yield $\theta_{xx} \simeq (t_0 - t)^{\alpha-2}\Theta''$, we can deduce

$$\alpha = 2 + \frac{1}{\gamma}.$$

This implies, from our numerical results, that in the case $\delta = \frac{1}{2}$, $\alpha \simeq 2 - \frac{1}{0.627} = 0.4051$. In figure 5, we represent the values of γ such that κ^γ fits best a straight line as a function of δ. Note that γ decreases monotonically up to the value $\gamma = -\frac{2}{3}$ for $\delta = 1$ which would follow from our explicit self-similar solution constructed above.

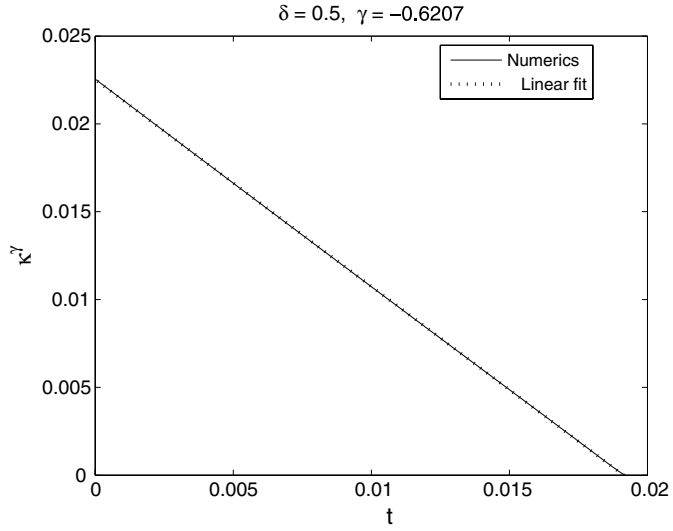

Figure 4. Evolution of the maximum curvature raised to the power γ. The exponent γ is chosen so that we get the best fit to a straight line. $\delta = 0.5$.

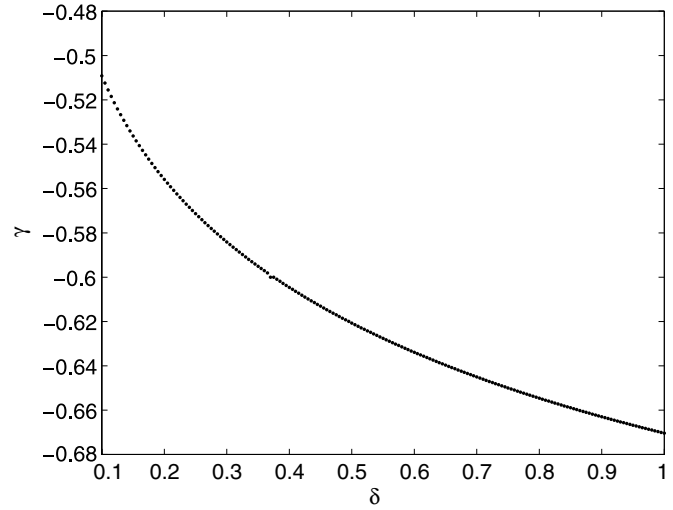

Figure 5. Exponent γ as a function of δ.

4. The case $\delta = 0$

This is a singular limit since the maximum of θ does not move and remains with the same value (say $\theta_{\max} = \theta_0$) all the time. The singular solutions might have a self-similar form of the type

$$\theta(x,t) = \theta_0 - (t_0 - t)^{\beta-1}\Theta\left(\xi \equiv \frac{x - x_0}{(t_0 - t)^{\beta}}\right), \tag{28}$$

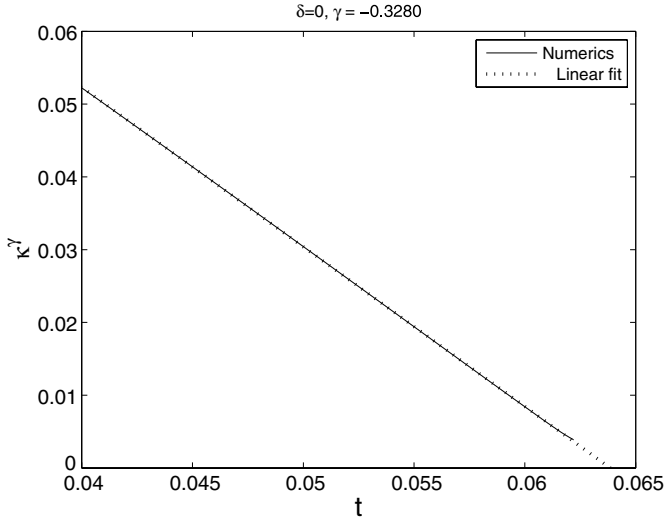

Figure 6. Evolution of the maximum curvature raised to the power γ. The exponent γ is chosen so that we get the best fit to a straight line. $\delta = 0$.

where $\beta > 1$ is a free parameter to be fixed with the condition

$$\Theta(\xi) \sim A|\xi|^{\frac{\beta-1}{\beta}} \qquad \text{as} \quad \xi \to \pm\infty\,. \tag{29}$$

The asymptotics (29) implies

$$\theta(x,t_0) \simeq \theta_0 - A\,|x-x_0|^{\frac{\beta-1}{\beta}} \qquad \text{as} \quad x \to x_0.$$

Our results represented in figure 6 indicate that the value of γ such that κ^γ fits best a straight line is -0.3280 . From (28), it follows that $\theta_{xx} \simeq -(t_0-t)^{-2\beta-1}\Theta''$ so that $\beta = -\frac{1}{2} + \frac{1}{2\gamma} \simeq 2.04488$. This value of β is so close to 2 that we conjecture it as exactly equal to 2.

In order to support our conjecture, we have verified numerically some of its consequences starting with the initial data $\theta(x,0) = 2\mathrm{sech}(15(x-\pi))$. We have computed the profiles of $\theta(x,t)$ for several times close to the formation of the singularity (see figure 7) and represented the profiles of $\Theta \equiv (\theta_0 - \theta(x,t))/(t_0-t)$ as a function of $\xi \equiv (x-\pi)/(t_0-t)^2$ in figure 8. We can see the collapse to a curve with a sublinear growth at infinity. In fact, from (28) and for $\beta = 2$, it will follow a growth $\Theta(\xi) \sim A|\xi|^{\frac{1}{2}}$.

Another observation concerns the Hilbert transform of $\theta(x,t)$; note that for the self-similar solutions

$$H\theta = -(t_0-t)(H\Theta)(\xi) = -(t_0-t)\frac{1}{\pi}PV\int_{-\infty}^{\infty}\frac{\Theta(\xi\xi'')}{1-\xi''}\,\mathrm{d}\xi''$$

$$\approx -(t_0-t)\frac{\mathrm{sign}(\xi)}{\pi}PV\int_{-\infty}^{\infty}\frac{A\,|\xi|^{\frac{1}{2}}\,|\xi''|^{\frac{1}{2}}}{1-\xi''}\,\mathrm{d}\xi'' = -(t_0-t)A\,|\xi|^{\frac{1}{2}}\,, \quad \text{for} \quad |\xi| \gg 1.$$

Hence $[(H\theta)^2]_x = [(H\Theta)^2]_\xi \approx \mathrm{sign}(\xi)A^2$, for $|\xi| \gg 1$ and therefore the profiles $[(H\theta)^2]_x$ as a function of $\xi \equiv (x-\pi)/(t_0-t)^2$ should converge, as $t \to t_0$, to a profile $[(H\Theta)^2]_\xi$ that tends to constant values as $|\xi| \to \pm\infty$. In figure 9, we can see that this is indeed the case.

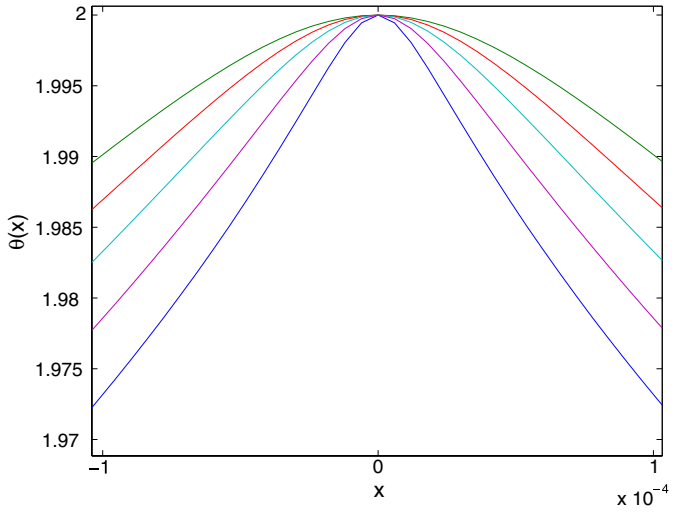

Figure 7. Profiles of θ near its maximum (at $x = \pi, \theta = 2$) for times $t_i = 0.0035, 0.003, 0.0025, 0.0020, 0.0015$ away from the singularity.

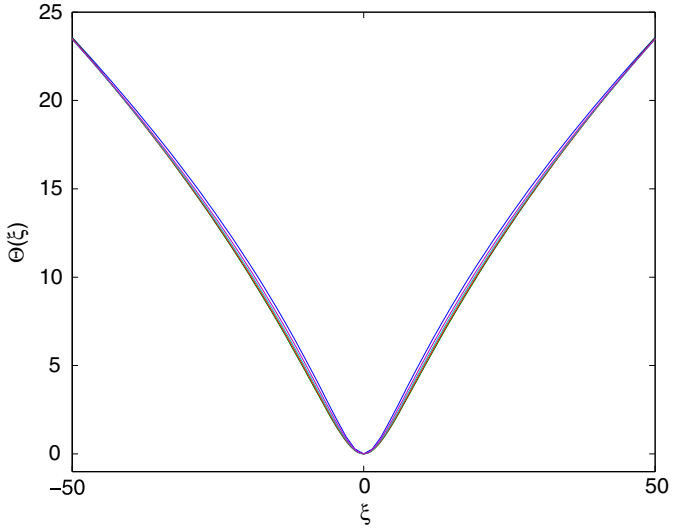

Figure 8. Rescaled profiles of $\theta_0 - \theta$ at times $t_i = 0.0035, 0.003, 0.0025, 0.0020, 0.0015$ previous to the formation of the singularity.

Finally, we remark that the development of a singularity in the form $\theta(x, t_0) = \theta_0 - A|x - x_0|^{\frac{1}{2}}$ allows a simple continuation of the solution *after* the singular time, i.e. for $t > t_0$. This continuation is given by the explicit solution of (5)

$$\theta(x, t) = \theta_0 - \tfrac{1}{2}A^2(t - t_0) - A|x - x_0|^{\frac{1}{2}}, \tag{30}$$

as one can simply check from the fact that

$$H\theta = H(-A|x - x_0|^{\frac{1}{2}}) = A\,\mathrm{sign}(x)|x - x_0|^{\frac{1}{2}},$$

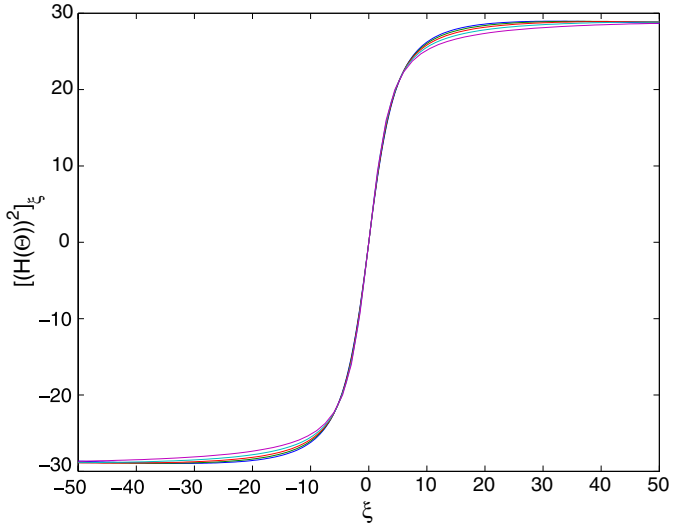

Figure 9. Rescaled profiles of $[(H\theta)^2]_x$ at times $t_i = 0.0035, 0.003, 0.0025, 0.0020, 0.0015$ previous to the formation of the singularity.

$$\theta_x = -\frac{A}{2}\text{sign}(x)|x - x_0|^{-\frac{1}{2}}, \qquad \theta_t = -\frac{1}{2}A^2.$$

For general initial data, one can continue the solutions after the singularity with a singular solution that behaves locally near the singularity in the form

$$\theta(x,t) = \theta_0 - \frac{1}{2}\int_{t_0}^{t} A^2(\tau)\,\mathrm{d}\tau - A(t)|x - x_0|^{\frac{1}{2}},$$

with $A(t)$ chosen appropriately so as to match the solution outside the region of formation of the singularity.

5. Numerical method

Our numerical experiments involve integration of the equation

$$\begin{aligned}\theta_t &= \delta(\theta H(\theta))_x + (1-\delta)H(\theta)\theta_x \\ &= \delta\theta H(\theta_x) + H(\theta)\theta_x,\end{aligned}$$

with $\delta \in [0,1]$, $x \in [0, 2\pi]$, $t > 0$. We use the classical fourth-order Runge–Kutta method in time. Since the support of $\theta(x,t)$ is very concentrated for the kind of initial data we use, we consider $\theta(x,t)$ to be periodic in our numerical simulations. Then, we represent it by means of its frequencies

$$\theta(x,t) = \sum_{\xi=-N/2}^{N/2-1} \hat{\theta}(\xi,t)\,\mathrm{e}^{\mathrm{i}\xi s}.$$

The conversion between $\theta(x_j,t)$, with $x_j = \frac{2\pi}{N}j$, and $\hat{\theta}(k,t)$, with $k = -\frac{N}{2},\ldots,\frac{N}{2}-1$ has been made by means of the fast Fourier transform (FFT), where N is chosen to be

a power of 2. That enables us to spectrally calculate θ_x, $H\theta$ and $H\theta_x$. In particular, $H(\theta(x,t)) = \sum_{\xi=-N/2}^{N/2-1} -\mathrm{i}\,\mathrm{sign}(\xi)\hat{\theta}(\xi,t)\,\mathrm{e}^{\mathrm{i}\xi x}$. In the numerical experiments presented in sections 3 and 4, we have considered the initial datum $\theta(x,0) = 2\mathrm{sech}(15(x-\pi))$ for $x \in [0, 2\pi]$. We have implemented all our experiments with $N = 262144$. Δt used has been $\Delta t = 10^{-5}$. We have considered 201 uniformly distributed values for δ, i.e. $\delta = 0$, $0.005, 0.01, 0.015, \ldots, 1$.

The singularity time gets smaller as δ increases, ranging from $t_{\max} \approx 0.12$, when $\delta = 0$, to $t_{\max} \approx 0.02$, when $\delta = 1$. Our assumption is that $\max|\theta_{xx}(t)| = t^{\frac{1}{\gamma}}$, when t approaches the singularity time. Given a γ in that interval, we try to adjust $(\max|\theta_{xx}(t)|)^{\gamma}$ to a straight line, calculating that line by the least-square method. We remark that for the theoretically known case, $\delta = 1$, we have obtained $\gamma = -0.6661$, i.e. a value extremely close to the exact $\gamma = -2/3$. From our numerical experiments, γ appears to be independent of the initial data.

References

[1] Córdoba A, Córdoba D and Fontelos M A 2005 Formation of singularities for a transport equation with nonlocal velocity *Ann. Math.* **162** 1375–87

[2] Chae D, Córdoba A, Córdoba D and Fontelos M A 2005 Finite time singularities in a 1D model of the quasi-geostrophic equation *Adv. Math.* **194** 203–23

[3] Córdoba A, Córdoba D and Fontelos M A 2006 Integral inequalities for the Hilbert transform applied to a nonlocal transport equation *J. Math. Pure Appl.* **86** 529–40

[4] Baker G R, Li X and Morlet A C 1996 Analytic structure of 1D-transport equations with nonlocal fluxes *Physica* D **91** 349–75

[5] Constantin P, Majda A J and Tabak E 1994 Formation of strong fronts in the 2-D quasigeostrophic thermal active scalar *Nonlinearity* **7** 1495–533

[6] Held I, Pierrehumbert R, Garner S and Swanson K 1995 Surface quasi-geostrophic dynamics *J. Fluid Mech.* **282** 1–20

[7] Holm D D and Putkaradze V 2007 Formation and evolutions of singularities in anisotropic geometric continua *Physica* D **234** 33–47

[8] Morlet A 1998 Further properties of a continuum of model equations with globally defined flux *J. Math. Anal. Appl.* **221** 132–60

[9] Ohkitani K and Yamada M 1997 Inviscid and inviscid-limit behavior of a surface quasi-geostrophic flow *Phys. Fluids* **9** 876–82

[10] Pedlosky J 1987 *Geophysical Fluid Dynamics* (New York: Springer)

[11] Resnick S 1995 *Dynamical problems in nonlinear advective partial differential equations* PhD Thesis *University of Chicago, Chicago*

[12] Stein E 1970 *Singular Integrals and Differentiability Properties of Functions* (Princeton, NJ: Princeton University Press)

[13] Wu J 1997 Inviscid limits and regularity estimates for the solutions of the 2-D dissipative Quasi-geostrophic equations *Indiana Univ. Math. J.* **46** 1113–24